

Supporting information

Sensitive SERS detection of miRNA using a label-free multifunctional probe

Hao Zhang,^a Yu Liu,^a Jian Gao,^{*a} and Junhui Zhen^{*b}

^a Department of Chemistry, Qilu University of Technology, Jinan 250353, China.

E-mail: gaojian@qlu.edu.cn

^b School of Medicine, Shandong University, Jinan 250012, China. E-mail:

zhen6576@126.com

Table of Contents

Experimental section.....	S3
Characterization of AuNPs.....	S6
Figure S-1.....	S6
UV-visible spectra of the ROX-DNA conjugates.....	S6
Figure S-2.....	S7
Optimization of the experimental conditions.....	S7
Figure S-3.....	S7
Figure S-4.....	S8
Figure S-5.....	S9
Figure S-6.....	S10
Figure S-7.....	S11
Figure S-8.....	S12
Figure S-9.....	S13
Table S-1. Oligonucleotide sequences used in our experiments.....	S15
Table S-2. The comparison of different methods for miRNA detection.....	S15
References.....	S17

EXPERIMENTAL SECTION

Materials and Reagents: All oligonucleotides designed in this study were synthesized by Sangon Biotech Co., Ltd. (Shanghai China); their sequences are listed in Table 1. Magnetic microbeads (MBs) modified with carboxyl group (1.0-2.0 μm , 10 mg/mL) were commercially available from Baseline ChromTech Research Center (Tianjin, China). 1-Ethyl-3-(3-dimethylaminopropyl) carbodiimide (EDC) and Chloroauric acid ($\text{HAuCl}_4 \cdot 3\text{H}_2\text{O}$) were obtained from Sigma-Aldrich (St. Louis, MO). The washing buffer was phosphate-buffered saline (PBS) solution (10 mM phosphate buffer, 0.14 M NaCl, 2.7 mM KCl, pH 7.4). Nicking endonuclease (Nt.A1wI) and Klenow polymerase by Sangon Biotech Co., Ltd. (Shanghai China), 0.45 $\text{U}\mu\text{L}^{-1}$, respectively. The hybridization chain reaction buffer was Tris buffer (20 mM, pH 7.6) containing 300 mM NaCl and 50 mM MgCl_2 . All chemicals employed were of analytical grade and used without further purification. Doubly distilled deionized water was used throughout the experiments.

Apparatus: Scanning electron microscopy (SEM) images were taken with a JEM 1200EX transmission electron microscope (JEOL, Japan). UV/Vis absorption spectra were obtained with a Cary 50 UV/Vis-NIR spectrophotometer (Varian, USA). SERS was performed on an inVia Raman microscope (Renishaw, England).

Preparation of Gold Nanoparticles (AuNPs): AuNPs were synthesized by reduction

of tetrachloroauric acid (HAuCl₄) with trisodium citrate. Briefly, 100 mL of 0.01% (w/w) HAuCl₄ solution was boiled with vigorous stirring, and then 1.5 mL of 1% (w/w) trisodium citrate solution was rapidly added to the boiling solution. The resulting reaction solution was maintained at its boiling point for 30 min. The color of the solution changed from faint-yellow to purple before a wine-red color was reached, indicating the formation of AuNPs. The resulting colloidal suspension was allowed to naturally cool to room temperature with continuous stirring. The synthesis of AuNPs was characterized by SEM (Figure S-1). The prepared gold colloidal solutions were stored in brown glass at 4 °C until use.

Preparation of AuNP-functionalized Raman Probe: The Raman-probe functionalized AuNPs were prepared as follows. Briefly, 10 μL of 1×10⁻⁷ M 5'-thiol modified capture DNA and 50 μL of 1×10⁻⁶ M bio-barcode (5'-thiol and 3'-Rox) was added to freshly prepared AuNPs (1 mL), and shaken gently overnight (approximately 20 h) at 37 °C. Subsequently, the DNA-AuNPs conjugates were aged in 0.05 M salts (NaCl, 200 μL) for 6 h and in 0.1 M salts (NaCl, 200 μL) for 6 h, respectively. Excess reagents were removed by centrifugation at 10,000 rpm for 30 min. After the supernatant was removed, the red precipitate was washed and centrifuged three times. The resulting bio-barcode probe was finally dispersed into 100 μL of 0.01 M pH 7.4 phosphate buffer (PBS, 0.01 M, pH 7.4) and stored at 4 °C

Immobilization of Hairpin capture DNA (Hc) onto MBs: Hairpin DNA was heated at the water bath 90 °C for 5 min and then allowed to cool to room temperature for 1 h before use. First, a 20 μL suspension of carboxylated MBs were placed in a 0.5 mL

Eppendorf tube (EP tube) and separated from the solution on a magnetic rack. After the MBs were washed three times with 200 μL of 0.1 M imidazol-HCl buffer (pH 6.8), they were activated in 200 μL of 0.1 M imidazol-HCl buffer (pH 6.8) containing 0.1 M EDC at 37 $^{\circ}\text{C}$ for 30 min. After been washed three times with 200 μL of 0.01 M PBS (pH 7.4), 20 μL of 1 M Hcs were separately added to the freshly activated MBs and incubated at 37 $^{\circ}\text{C}$ overnight. Finally, the excess DNAs were removed by magnetic separation. The resulting DNA-conjugated MBs were rinsed three times with 200 μL of 0.01 M PBS (pH 7.4), resuspended in 200 μL of 0.01 M PBS and stored at 4 $^{\circ}\text{C}$ for use.

Assay Procedure of miR-203: The miR-203 analysis was carried out as follows: Firstly, the probe was heated at the water bath 90 $^{\circ}\text{C}$ for 5 min and allowed to cool to room temperature for 1 h. Then, miR-203 samples at specific concentration (5 μL), primer (1 μM , 10 μL) and Klenow polymerase (1.0 μL), dNTPs (5 μL) and Nt.AlwI (1 μL) in NEBuffer were added into the heated aptamer solution(10 μL). The concentrations of nicking endonuclease (Nt.AlwI) and Klenow polymerase were 0.45 $\text{U}\mu\text{L}^{-1}$ (1 μL in 5 μL buffer), respectively. Finally, the whole system was incubated for 2 h at 37 $^{\circ}\text{C}$. After that, the reacted solution and bio-bar code (10 μL) were added into DNA-conjugated MBs for 2 h at 37 $^{\circ}\text{C}$. Then the MBs incorporated Raman probes were performed through magnetically controlled separation to remove the excess bio-barcode, washed with PBS for three times and redispersed in 20 μL of 0.01 M PBS (pH 7.4, 0.3 M NaCl) .

SERS Measurements: Two microliters of the MB-incorporated Raman molecular

probe solution was pipetted onto the surface of gold film (glass slide with gold plating) and air-dried at room temperature. Raman spectra were measured using a Raman spectrometer at an excitation laser of 633 nm. The laser power was 5 mW. The acquisition time for each spectrum was 10 s. Eleven spectra were obtained from different sites of each sample and averaged to represent the SERS results, and the experiments were carried out in triplicate. Error bars show the standard deviation of the eleven experiments.

RNA extraction and quantitative real-time PCR (qRT-PCR) assay:

Total RNA was extracted from 10^7 cells while RNA enriched in small molecules was obtained using the Ambion reagent (Invitrogen) in accordance with the manufacturer's instructions (Applied Biosystems). RNA concentration was measured with NanoDrop (Implen). The expression level of mature miR-203 was measured by real time PCR with HiScript II One Step QRT-PCR SYBR Green Kit (Vazyme). The threshold cycle (CT) is defined as the fractional cycle number at which the fluorescence passes the fixed threshold (Figure S-5). Experiments were performed in triplicate for each data point, and data analysis was performed by use of 7500-Fast Software v2.3.

Characterization of AuNPs: The AuNPs synthesized were characterized by SEM (Figure S-1).

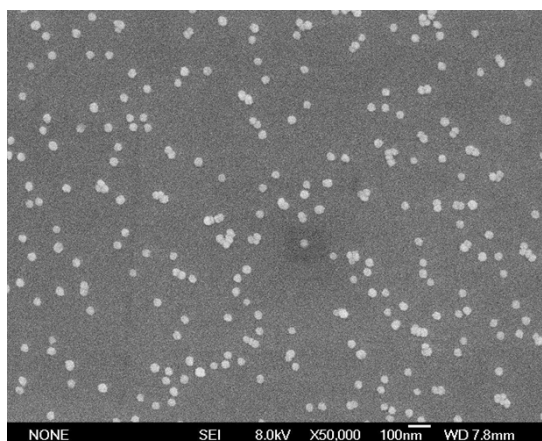


Figure S-1. SEM image of AuNPs synthesized (approximately 25 nm)

UV-visible spectra of the Rox-DNA conjugates: The UV-visible spectra of capture DNA probe, AuNPs, signal probe (Rox-DNA) and SERS bio-bar codes (SERS signal probes) were carried out on a Cary 50UV/Vis spectrophotometer. As revealed in Figure S-2, the curve a showed the characteristic absorbance of signal probe (~260 nm and 500~600 nm, respectively, DNA characteristic absorbance and Rox characteristic absorbance). Curve b exhibited the AuNPs characteristic absorbance (~520 nm) and Curve c showed the characteristic absorbance of capture DNA probe (~260 nm). Curve d revealed both the characteristic absorbance of AuNPs, DNA and Rox which meant the successful conjugation of Rox-DNA with AuNPs, to be called SERS bio-barcodes. The results in Figure S-2 .

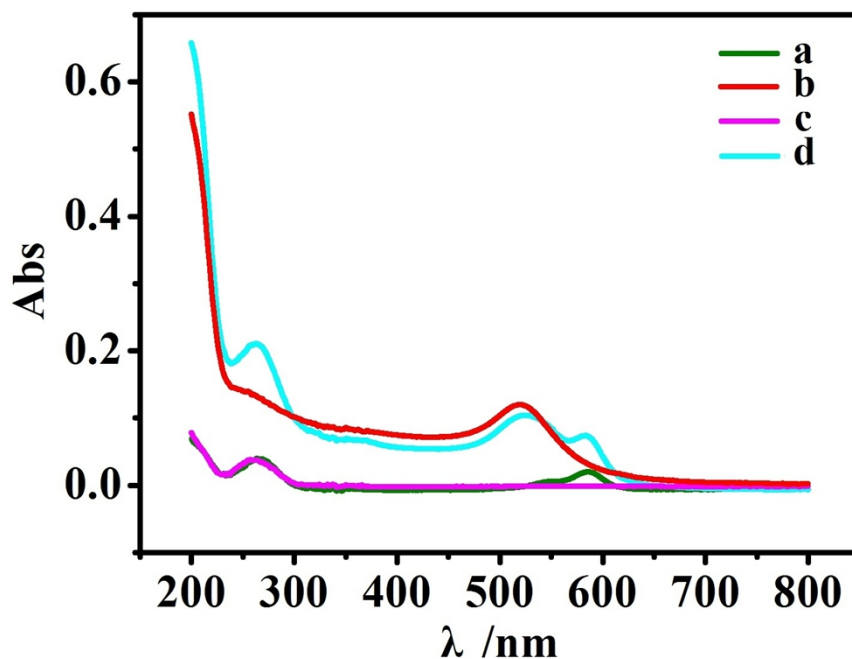


Figure S-2. UV spectra of a) Rox-DNA, b) capture DNA probe, c) AuNPs and d) SERS bio-barcode.

Optimization of the sequences of the smart probe: To obtain the best performance of the sensing system, the sequence of the smart probe with hairpin structure was optimized. We designed five different hairpin probes (probe 1, probe 2, probe 3, probe 4, probe 5) that included 7, 9, 11, 13 and 15 base pairs in the region 3 (the stem of the hairpin), respectively (Table S1). The thermodynamic properties of five probes sequences were measured. An increase of the base pairs in the region 3 from 7 (probe 1) to 15 (probe 3) resulted in a high melting temperature of suggesting that the more base pairs in the region 3 could facilitate the stability of the probe. However, further increase of the base pairs in the region 3 from 4 (probe 2) to 5 (probe 4) might result in a high melting temperature, which shows a weak ability to hybridize with target RNA and reduced the recognition sensitivity, therefore, probe 3 was then chosen in further experiments. Moreover, the intensities of Raman signal with the probes were

.investigated. As shown in Figure S-3, the Raman intensity (ΔI) reached a maximum with the probe 3, thus, we selected probe 3 as the optimum probe.

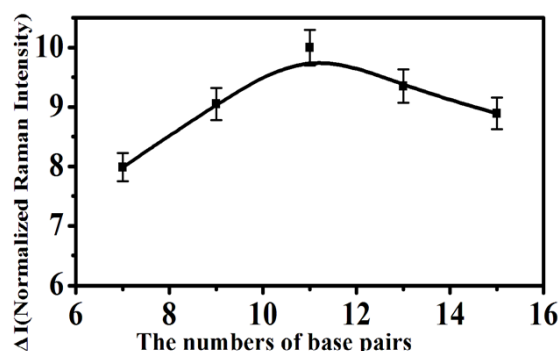


Figure S-3. Influence of the numbers of base pairs, on the ΔI signal (miR-203, 10^{-13} M).

Optimization of the reaction temperature and pH: The temperature and pH of reaction solutions strongly influence DNA hybridization and the activity of enzyme. So they are the two most important parameters for optimizing the analysis system. We therefore investigated the intensity of Raman signal under different temperature and pH conditions. The influence of pH values ranging from 5.5 to 9.0 for the Raman-signal intensity produced by 1.0×10^{-13} M miR-203 in Figure S-4A, the Raman intensity (ΔI) reached a maximum at pH 7.4. Thus, we selected pH 7.4 as the optimum condition.

As shown in Figure S-4B, the Raman intensity (ΔI) increased with the temperature from 20 °C to 50 °C, which reached a maximum at 37 °C. After that, the intensity decreased gradually. Thus, 37 °C was chosen as the optimal temperature.

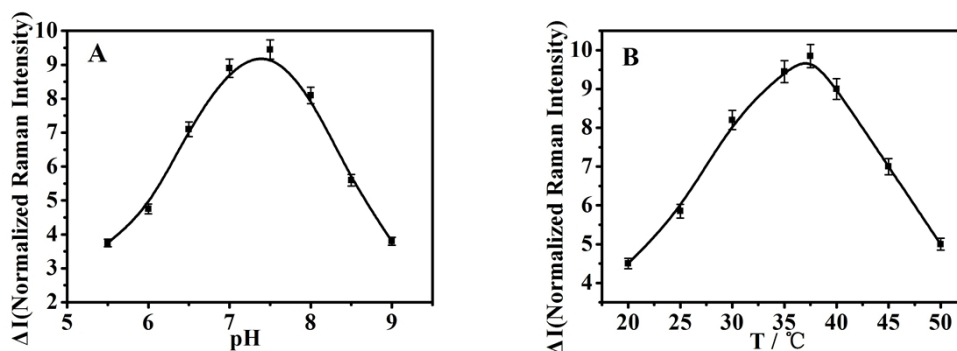


Figure S-4. Influence of pH (A) and temperature (B) of the reaction, on the ΔI signal (miR-203, 10^{-13} M).

Optimization of the incubation time: The incubation time was investigated. Figure S-5 shows the changes of Raman signals generated by performing the experiments at different time intervals. The results revealed that the Raman intensity increased rapidly as the incubation time prolonged and reached a plateau after 100 min. We therefore deduced that 100 min was the best incubation time for the assay.

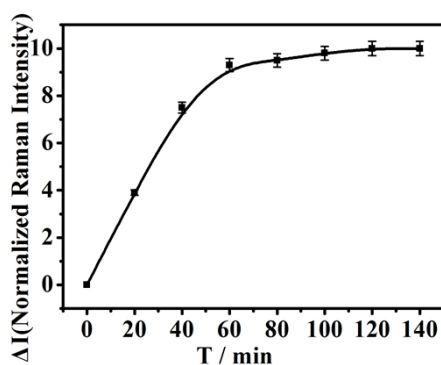


Figure S-5. Effect of the time of the reaction on the ΔI signal (miR-203, 10^{-13} M)

Optimization of the amount of nicking endonuclease and Klenow polymerase: The amount of nicking endonuclease and Klenow polymerase have effected on the Raman intensity. To increase the sensitivity of Raman detection, we designed a series of control experiments to optimize the amount of Nt.AlwI and Klenow polymerase.

The results demonstrated that the Raman intensities enhanced rapidly with the increase of the amount of Nt.AlwI up to $0.45 \text{ U}\mu\text{L}^{-1}$ (Figure S-6A), followed by a plateau. Therefore $0.45 \text{ U}\mu\text{L}^{-1}$ of Nt.AlwI was adopted to be the optimum amount for the system polymerization. Similarly, as it could be seen in Figure S-6B, $0.45 \text{ U}\mu\text{L}^{-1}$ of the polymerase was the optimum.

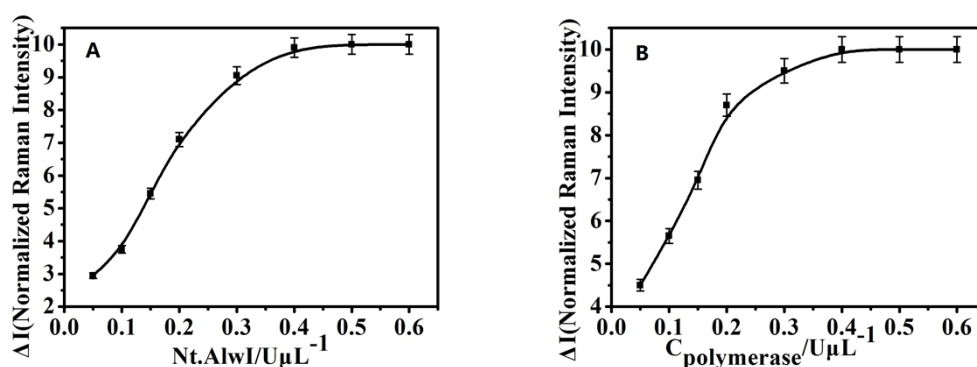


Figure S-6. Effect of the amount of nicking endonuclease (A) and the Klenow polymerase (B) on the ΔI signal (miR-203, 10^{-13} M).

Optimization of the concentration of the hairpin DNA immobilized on the MB and the proportion of the signal probes and the capture probe immobilized on the Au-NPs: The Raman intensity is also influenced by the proportion of the signal DNA probes and the capture probe immobilized on the Au-NPs in the preparation of bio barcode probe. To improve the sensitivity of SERS quantification of DNA, the proportion of the capture probe and the signal DNA probes was optimized. Figure S-7A shows the variance of Raman intensity with the proportion of the signal DNA probes and the capture probe. It was obviously that Raman intensity increased upon raising the proportion from 30:1 to 50:1, and then it started to level off, attributed to the steric and electrostatic hinderance arising from the more tightly packed probe,

which were necessary for highly hybridization efficiency. Thus the ratio of 50:1 was selected for the subsequent assays. Figure S-7B shows the variance of SERS intensity with the concentration of hairpin probes. It can be seen that the SERS intensity increases with the increase of hairpin DNA concentration from 1.0×10^{-9} M to 1.0×10^{-5} M, and reaches a maximum at 1.0×10^{-7} M, upon analyzing target RNA at a concentration corresponding to 1.0×10^{-13} M. These results demonstrated that low concentration hairpin probes might not hybridize with sufficient target RNA, but high-concentration hairpin probes might increase the steric hindrance of the microenvironment, adversely preventing their hybridization with target RNA. Therefore, the concentration hairpin probes of 1.0×10^{-7} M was employed in the following work.

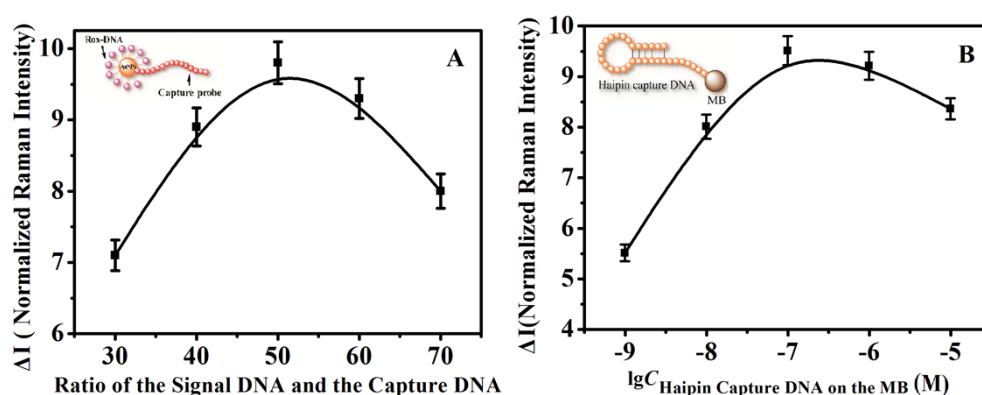


Figure S-7. (A) Effect of the concentration of the hairpin DNA immobilized on the MB on the ΔI signal. (B) Effect of the proportion of the signal probes and the capture probe immobilized on the Au NP on the ΔI signal. (miR-203, 10^{-13} M).

The Selectivity for RNA detection: To evaluate the detection specificity of the current assay, the SERS intensity with T2 (non complementary RNA, column A), T3 (One base mismatched RNA, column B), T1 (target RNA, column C) and target RNA

(in presence of 10^{-10} non complementary RNA, column D) were presented in the concentration respectively for 10^{-14} M, 10^{-13} M, 10^{-12} M. From Figure S-8, it can be seen that in the presence of non complementary RNA, no significant difference in SERS signals was observed as compared to the control group without target RNA. The cycle 1 was not initiated, and Ts as primer probe was not released, the cycle 2 did not happened. Accordingly to the column C, the one-base mismatched RNA produced a 60% lower analytical signal in comparison with the full matching target RNA in the presence of 10^{-12} M. In addition, No obvious difference in the SERS intensity of column D and column E, is suggesting the excess RNA had no significant effect on the detection of target RNA. All the analysis shows the present method has a good specificity for RNA detection.

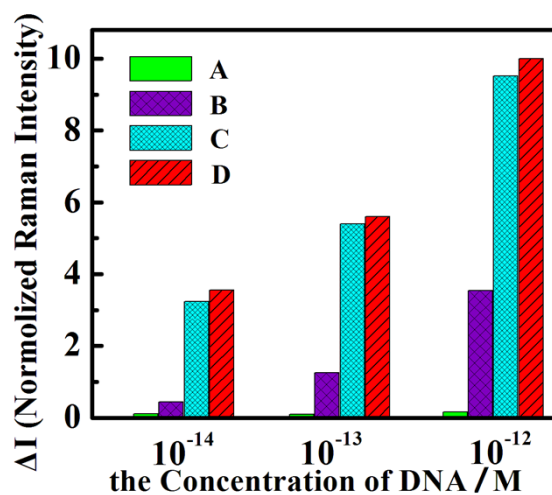


Figure S-8. Specificity for the detection of RNA against non complementary RNA (miRNA-200), one base mismatched RNA, miR-203 and miR-203 (in presence of 10^{-10} miRNA-200), in the concentration respectively for 10^{-14} M, 10^{-13} M, 10^{-12} M. Normalized Raman intensity in presence of miRNA-200, column A, one base mismatched RNA, column B, miR-203, column C and miR-203 (in presence of 10^{-10} miRNA-200), column D. The blank was subtracted for each value.

The Quantitative real-time fluorescence monitoring of the qRT-PCR reactions:

To investigate the comparison between our method and the conventional RT-PCR, we also investigated the sensitivity of the conventional method by testing the same RNA (T1). S-9A, B indicates that the detection range of the conventional method is from 500 fM to 5 nM, and the correlation equation is $\Delta C_T = 2.01611 \lg C_{T1} + 48.8086$, with an R^2 of 0.9985. It is clearly seen that the conventional method gives a poorer performance in sensitivity, dynamic detection range, and linear relationship between target concentration and ΔC_T value when compared with our method.

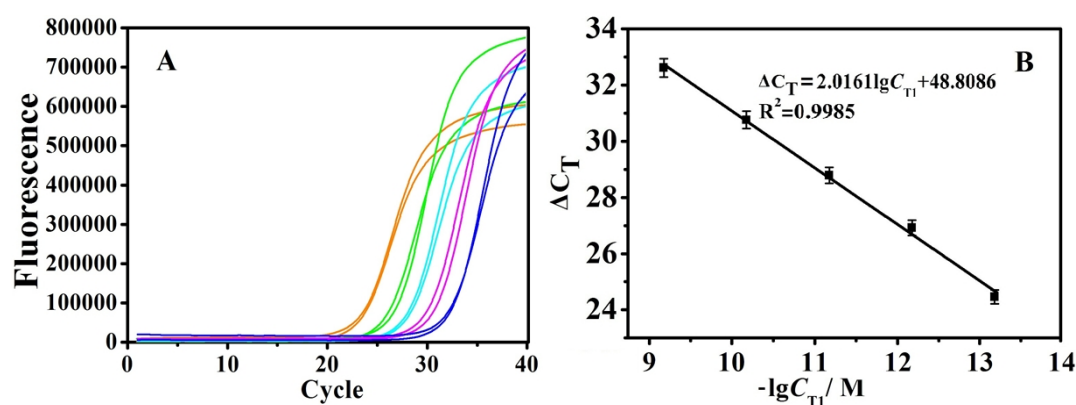


Figure S-9. (A) Quantitative real-time fluorescence monitoring of the qRT-PCR reactions triggered by miR-203 at different quantity. RFU represents the fluorescence units. (B) Plot of the relationship between ΔC_T value and the logarithm of the concentration of miR-203 (T1) based on the data (A)

Table S-1. Oligonucleotide sequences used in our experiments.

Oligonucleotide name	Sequences (5' to 3')
Probe 1	AGCTGTAGTTGGCCCTCAGATCCCTAGTGGT CCTAAACATTTACAGGCACTACAG ATAGGA
Probe 2	AGCTGTAGTCGTGGATCAGATCCCTAGTGG TCCTAAACATTTACAGGCACTACAG ATAGGA
Probe 3 (Smart multifunctional probe)	AGCTGTAGTGCCTCCTCAGATCCCTAGTGGT CCTAAACATTTACAGGCACTACAG ATAGGA
Probe 4	ATCTGTAGTGCCTCCTCAGATCCCTAGTGGT CCTAAACATTTACAGGCACTACAG ATAGGA
Probe 5	CTATCTGTAGTGCCTCCTCAGATCCCTAGTG GTCCTAAACATTTACAGGCACTACAG ATAGGA
Primer DNA	TCC TAT CTG TAG
Hairpin capture DNA (Hc)	NH ₂ -TTTTTT- AGCTGTAGTGCCTCATGACGTACAGC
Capture DNA	SH-GCT GTA CGT CAT
Signal DNA	Rox-TTTTTTCCTAGCGAC-SH
Hsa-miR-203	GUG AAA UGU UUA GGA CCA CUA G
one-base mismatched miRNA	GUG AAA UGU UUA <u>G</u> CA CCA CUA G
miRNA-200	UGU AGC AAU GGU CUG UCA CAA U

Table S-2. The comparison of different methods for miRNA detection

Method	Transducer	Detection limit
used as templates for copper nanocluster (CuNC)	electrocatalysis	8.2 fM ¹
catalyzed hairpin assembly reaction (CHA) and hybridization chain reaction (HCR)	celectrochemistry	10 fM ²
padlock probe-based exponential rolling circle	amperometry	6 pM ³

amplification (PERCA)		
Using bifunctional strand displacement amplification-mediated hyperbranched rolling circle amplification	Fluorescence	0.18 pM ⁴
Using hairpin probe-based rolling circle amplification (HP-RCA)	Fluorescence	10 fM ⁵
using a hemin-G-quadruplex complex as the sensing element	electrochemistry	4 pM ⁶
Colorimetric sensing method on the basis of the plasmonic coupling effect	colorimetry	1 pM ⁷
Using quadratic isothermal amplification	fluorescence	10 fM ⁸
Fluorescence quenching of gold nanoparticles integrating with a conformation-switched hairpin oligonucleotide probe	fluorescence	0.01 pM ⁹
Exponential amplification reaction (EXPAR)	SERS	0.5 fM ¹⁰
EXPAR	fluorescence	10 fM ¹¹
This work	SERS	6.3 fM

References

- 1 Z. Y. Wang, L. Si, J. C. Bao and Z. H. Dai, *Chem. Commun*, 2015, **51**, 6305.
- 2 Y. Cheng, J. P. Lei, Y. L. Chen and H. X. Ju, *Biosens. Bioelectron*, 2014, **51**, 431.
- 3 Y. Zhou, Z. Zhang, Z. Xu, H. Yin and S. Ai, *New J. Chem*, 2012, **36**, 1985.
- 4 L. Zhang, G. Zhu and C. Zhang, *Anal. Chem*, 2014, **86**, 6703.
- 5 Y. Li, L. Liang and C. Zhang, *Anal. Chem*, 2013, **85**, 11174.
- 6 Y. Zhou, M. Wang, X. Meng, H. Yin and S. Ai, *RSC Adv*, 2012, **2**, 7140.
- 7 J. Park and J.-S. Yeo, *Chem. Commun*, 2014, **50**, 1366.
- 8 R. X. Duan, X. L. Zuo, S. T. Wang, X. Y. Quan, D. L. Chen, Z. F. Chen, L. Jiang, C. H. Fan and F. Xia, *J. Am. Chem. Soc*, 2013, **135**, 4604.
- 9 Y. Tu, P. Wu, H. Zhang and C. Cai, *Chem. Commun*, 2012, **48**, 10718.
- 10 L. P. Ye, J. Hu, L. Liang and C. Y. Zhang, *Chem. Commun.*, 2014, **50**, 11883
- 11 M. Zhang, Y. Q. Liu, C. Y. Yu, B. C. Yin and B. C. Ye, *Analyst*, 2013, **138**, 4812.